Journal of Applied Horticulture, 26(1): 95-99, 2024
https://doi.org/10.37855/jah.2024.v26i01.18
Journal of Applied Horticulture
ISSN: 0972-1045

Evaluation of the photocatalytic efficiency of cobalt oxide-reduced graphene oxide-banana biochar hybrid composite towards the degradation of organic dyes and heavy metal Chromium (VI)

Amrita priyadarsini[1], Chirasmayee Mohanty[2], Nigamananda Das[2], Nandita Swain[1], Manasi Dash[3], Abinash Mishra[3], Pradip Kumar Jena[1]*and Spandan Nanda[1]

*[1]Department of Chemistry, College of Basic Science and Humanities, Odisha University of Agriculture and Technology, Odisha. [2]Department of Chemistry, Utkal University, Bhubaneswar 751004, Odisha. [3]Department of Genetics and Plant Breeding, Odisha University of Agriculture and Technology, Odisha. *E-mail: pradip_callme@yahoo.co.in, nanda.spandan56@gmail.com*

Abstract

For a realistic solution, the synthesis of a cost-effective and efficient photocatalyst for the environmental need is utmost essential. Here, a simple *in situ* hydrothermal method that is a type of "green synthesis" since it doesn't require harmful chemicals was used to synthesise the simple catalyst Co_3O_4/reduced graphene oxide/biochar (CBG). The Co_3O_4 nanoparticles are finely distributed over the sheets of reduced graphene oxide and biochar during the morphological examination, making the composite stable and appropriate for environmental applications. This catalyst was specifically used to create a Z-scheme heterostructure composite that significantly improves the Co_3O_4 and biochar/rGO photocatalytic performance when exposed to visible light. When it comes to dye and heavy metal Chromium (VI) degradation, the catalyst composite exhibited significantly greater catalytic efficacy compared to individual catalysts. The structural, morphological, and optical features of the CBG nanocomposite were primarily responsible for its exceptional visible light photocatalytic activity with a maximum kinetic rate constant. By optimising the catalyst ratio, the herein described technology can be used to create a promising photocatalyst for environment friendly and sustainable development.

Key words: Biochar, nanocomposites, photocatalysis, heavy metals, industrial dye, sustainable

Introduction

The lifeblood of contemporary society is fresh water that is readily available and sufficient in a decent amount. Since the turn of the twenty-first century, the finding on fresh water sources has taken on more significance. Everyone on Earth will find the future age of water scarcity and ease of access to fresh water problematic, but if it is not anticipated, it will be significantly more difficult (Han *et al.,* 2014). Recently, metal oxides based on graphene have drawn attention from all over the world because of their many potential applications in dye degradation, supercapacitors and other electrochemical energy storage devices (Luo *et al.,* 2013). In the modern world, environmental pollution has emerged as a major issue that is getting alarmingly dangerous for all forms of life on earth. One of the main issues facing the globe today is water pollution, which is caused by the discharge of trash from industries and chemical companies into water bodies that contains organic and carcinogenic chemical substances. Excessive piling of organic contaminants in water creates soil pollution, which has directly or indirectly adversely affected every form of life. These pollutants have been removed using a variety of treatment strategies *viz.,* adsorption, coagulation, photocatalysis, biodegradation (Ye *et al.,* 2019). The ability of photocatalysis to convert hazardous organic substances into non-toxic inorganic compounds making it as one of the strongest contenders among all which is employed for the purification of water. Since photocatalytic degradation produces no secondary contaminants, it is a crucial technique for waste water management. The catalysts are reusable and the procedure involved in the due process is quite affordable (Bedia *et al.,* 2019). The ability of a photocatalyst to synthesise free radicals produced with the participation of electrons and holes determines its photocatalytic activity (Xu *et al.*, 2019). An effective photocatalyst should possess a number of essential criterions *viz.,* a well-tuned band gap, chemical and photo stability, and a high affinity for light (Yuan *et al.,* 2013). A-Fe_2O_3, Bi_2WO_6, CuO and Cu_2O, ZnO, WO_3, TiO_2, Cr_2O_3, and V_2O_5 NPs are some of the reported catalysts. Nano-sized metal oxides have been demonstrated as effective photocatalytic materials with a relatively larger surface area and efficient recyclability (Lester *et al.,* 2012). Additionally, the material design has drawn a lot of attention (Laguna-Marco *et al.,* 2010). Inorganic nanomaterials can be exploited in a variety of domains of interest because of their outstanding qualities, such as their appealing optical, magnetic, and electrical properties (Liao *et al.,*2014). Basically, the optical and electrical properties of nanoparticles are stimulated by their size and shape, both of which can be changed by the production process (Pouretedal and Kiyani, 2014). This investigation has underscored the notable potential of Co_3O_4 material as a promising photocatalyst within the realm of transition metal oxides. Its ascendancy arises from its facile synthesis methods, robust chemical stability, versatile morphology, and aptitude for electrocatalytic applications.

Notably, Co_3O_4 materials manifest themselves as magnetic p-type semiconductors, distinguished by their cubic spinel structures. They proffer both direct and indirect band gaps of 2.10 eV and 1.60 eV, respectively. This manifold of intriguing attributes beckons forth graphene, a two-dimensional carbon allotrope, renowned for capturing significant scientific attention (Peng *et al.,*2017). The utility of graphene, particularly in tandem with metal oxide nanocomposites, has garnered fervent exploration across various domains, including catalysis, supercapacitors, electrochemical and gas sensors, and photonic energy conversion devices (Bankole *et al.,*2020).

This research advances a sophisticated one-pot methodology for the synthesis of a novel Co_3O_4/reduced graphene oxide/biochar composite photocatalyst, harnessing the inherent capabilities of banana biochar, reduced graphene oxide, and Co_3O_4 to synergistically optimize photogenerated electron manipulation. This composite catalyst under visible light excites water and oxygen, catalyzing environmentally benign oxidants like hydrogen peroxide. Simultaneously, it facilitates photodegradation and facile magnetic separation. A comprehensive suite of analytical techniques, including SEM, FTIR, XRD, and UV-vis, has been judiciously employed to scrutinize the intricate features of these pioneering photocatalysts. The photocatalytic prowess of the Co_3O_4/reduced graphene oxide/biochar composite has been impeccably validated through the degradation of methylene blue, malachite green, and chromium (VI). Noteworthy is the composite's harmonious and synergistic photocatalysis under visible light, conferring resistance to the quenching of hydroxyl radicals and thereby amplifying photocatalytic efficiency. The promising applications of these hybrid composites encompass the photodegradation of dyes prevalent in diverse industrial wastewater contexts.

Materials and methods

The primary raw material employed in this study was the pseudostem of banana (BP), procured from banana trees in the vicinity of Bhubaneswar, Odisha. Chemicals including Cobalt (II) Chloride hexahydrate ($CoCl_2 \cdot 6H_2O$), Sodium Carbonate (Na_2CO_3), Sodium nitrate ($NaNO_3$), Potassium permanganate ($KMnO_4$), Hydrogen peroxide (H_2O_2), Ethanol (C_2H_5OH), Potassium dichromate ($K_2Cr_2O_7$), Sulphuric acid (H_2SO_4), Graphite, Methylene blue (MB), and Malachite green (MG) dye were employed in the current investigation. Throughout the synthesis process, all aqueous solutions were meticulously prepared using double distilled water.

Preparation of biochar: Banana pseudostem biomass underwent a thorough cleansing with tap water followed by distilled water to eliminate surface contaminants. Subsequently, it was sectioned into smaller pieces and subjected to an oven at 100°C until it attained a consistent weight. The resulting dried biomass was finely powdered using a pulverizer equipped with a 250 mm sieve before being placed in a muffle furnace for pyrolysis under a continuous flow of N_2 gas, maintaining a temperature of 500°C for a duration of 1 hour, with a heating rate of 10°C/min.

Synthesis of graphene oxide: In a typical procedure, 46 mL of concentrated sulfuric acid was added to a mixture comprising 1 g of concentrated graphite powder and 1 g of NaNO3, all within an ice bath. Subsequently, after 15 minutes of stirring, 8 g of potassium permanganate was gradually introduced into the mixture. Once the $KMnO_4$ was fully incorporated, the mixture continued to be stirred at room temperature for a duration of two hours. To this mixture, 80 mL of distilled water was added and stirred for an additional hour. Finally, 200 mL of distilled water was introduced, followed by H2O2 until gas evolution ceased. The produced graphene oxide (GO) was then separated via centrifugation and subsequently dried at 70°C for future use (Koli *et al.*, 2018).

Synthesis of CO_3O_4/Biochar/rGO(CBG-X): A predetermined quantity of rGO and biochar was combined with 20 mL of distilled water in an ultrasonicator for one hour. Subsequently, 3g of $CoCl_2 \cdot 6H_2O$ and 1M Na_2CO_3 were introduced into the mixture while it underwent stirring. After an additional hour of stirring, a dense purple-colored solution emerged (Scheme 1). This mixture underwent hydrothermal treatment in Teflon-lined autoclaves for a duration of five hours at 120°C. The resultant slurry was meticulously rinsed with ethanol and water, followed by overnight drying in an oven at 80°C. The dry sample was then subjected to calcination at 350°C for 5 hours, ultimately yielding a powdered form of the dark-colored CBG. Various weight percentages of biochar/rGO (2, 5, 10) were incorporated, and the resulting composites were designated as CBG-X, where x= 0, 2, 5, 10.

Adsorption/photocatalytic activity of dyes/Cr(VI): The adsorption behavior of biochar, CBG-2, CBG-5, CBG-10, Co3O4, and rGO samples towards dyes in the absence of light was investigated using a thermostated water bath shaker at a constant temperature. Specified quantities of the samples were combined with 100 mL of dye solutions at varying concentrations in conical flasks. Following pH adjustment to appropriate values, the flasks were agitated for a predetermined duration. The nanoparticles (NPs) were extracted in 5 mL aliquots, subjected to centrifugation for separation, and the supernatant's absorbance was measured at wavelengths corresponding to the absorption maxima of the respective dyes. The amount of adsorbed dye (mg/g) on the sample was calculated using the mass balance equation (Equation 1), where C_e represents the final equilibrium concentration of the dye in the solution (mg/L), qe is the equilibrium adsorption capacity per gram of the adsorbent (mg/g), C_o is the initial dye concentration in the solution (mg/L), V is the total solution volume (mL), and W is the weight of the adsorbent (g).

$$q_e = \frac{C_o - C_e}{W} \times V \quad (1)$$

Similar methodologies were applied to assess Cr(VI) adsorption, with the residual Cr(VI) concentration determined through the diphenylcarbazide technique. Optimal pH values for sorption and adsorption isotherms were established for dye/Cr(VI) concentration and pH, respectively. To facilitate comparisons with biochar/rGO, the adsorption of dyes/Cr(VI) on CBG-10, CBG-5, and CBG-2 was also evaluated under identical conditions. UV-Visible spectra in solution were recorded and absorbance values quantified using an Agilent Cary 100 UV-visible spectrophotometer. A minimum of two identical adsorption/desorption experiments were conducted for each sample, with average results duly recorded.

The photocatalytic efficacy of biochar, CBG-2, CBG-5, CBG-10, Co_3O_4, and rGO samples was ascertained by monitoring the degradation of two dyes, Methylene blue (MB) and Malachite green (MG). Batch photocatalytic experiments were carried out within a cylindrical, double-walled photocatalytic reactor

equipped with continuous stirring and illuminated by visible light. The reactor was outfitted with a 125 W Hg light source. The catalyst was accurately weighed and dispersed in 100 mL of dye solution at the required concentration. The solution's temperature was maintained at 25.0±0.5°C by circulating water through the reactor's outer wall. At regular intervals, samples of the reaction solution were withdrawn, subjected to centrifugation, and the absorbance of the supernatant was determined at wavelengths of 620 nm for MG and 664 nm for MB. The degree of dye degradation was calculated using Equation 2, and all spectral measurements were conducted using an Agilent UV-Visible spectrophotometer.

$$\text{Degradation (\%)} = \frac{C_o - C_t}{C_o} \times 100 \quad (2)$$

The results of the adsorption and photocatalytic analysis showed that the integration of Co_3O_4 with (biochar and rGO), or 10 wt%, produces the best results.

Results and discussion

The experimental data from the XRD analysis to ascertain the structural properties of the biochar Co_3O_4 , rGO , and CBG-10 nanocomposites are shown in Fig. 1. According to Fig. 1(c), pure reduced GO depicts diffraction peaks at 24.4 and 43.2 that belongs to (002) and (111) crystal planes. Fig.1(a) depicts the mineralogical composition and mineral phases of banana-waste biochar were characterized by X-ray diffraction analysis. The mineral composition consisted of a long hump with such a centroid between 20 and 30 degrees. Fig-1 (b) shows the pristine Co_3O_4 diffraction peaks at 2θ= 19.00,31.2,36.8,44.8 and 59.36 are corresponds to (111),(220),(311),(400) and (511). (JCPDS# 01-073-1701).For CBG-X(CBG-10) composite fig-1 (d) ,the most important diffraction peaks for Co_3O_4 are detected. The XRD results show that the CBG-10 heterostructure formed without the presence of any

In the spectral region of 400–4000 cm^{-1}, Fig. 2 shows the typical FTIR spectrum of annealed Cobalt oxide nanoparticles, CBG-10, rGO, and biochar. Using the FTIR approach, the purity and metal quality of a material made of metal oxide were evaluated. One could see from Fig. 2 that the FTIR spectra of Co3O4 showed a notable aggregation of peaks at 572 cm^{-1} and 664 cm^{-1}. The Co-O shaking mode frequency was responsible for the peak at 572 cm^{-1}, whereas the O-Co-O bond's bridging shake was responsible for the peak at 664 cm^{-1}. C-O stretching vibrations could be the cause of the minor peak at 1118 cm^{-1}. The absorption of carbon during the thermal interaction of metal oxides with the atmosphere, which results in the appearance of peaks at 2345 cm^{-1}, could be the explanation for the asymmetric vibration (C=O) of CO_2. The C-N stretching of the benzene rings, which emerged from C-N stretching modes in conjugation, which commonly related to stretching vibrational modes from -NH groups and surface-adsorbed molecules of water, had a broad peak that ranged from 3000 to 3400 cm cm^{-1}. The intensity of the FTIR peak position decreased as Co_3O_4 material was added to biochar/reduced graphene oxide. The CBG-10 material contained an interaction between Co_3O_4 and biochar/reduced graphene oxide in proportion to these findings, which is also compatible with the XRD data.

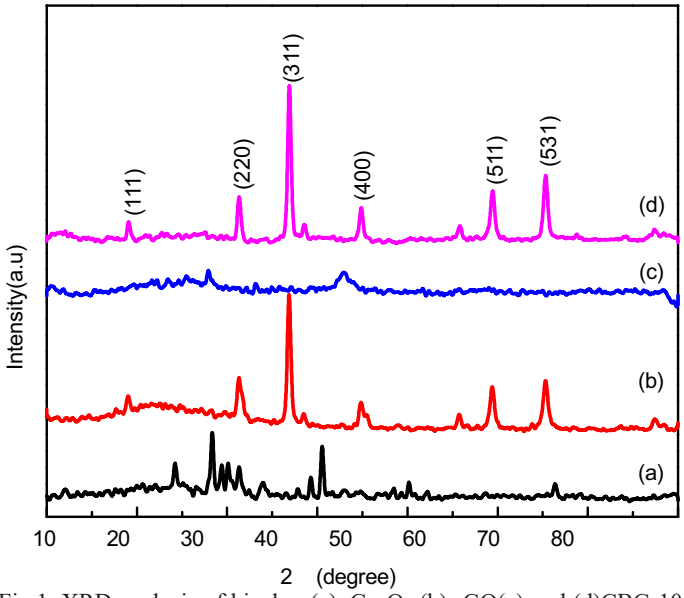

Fig.1. XRD analysis of biochar (a), Co_3O_4 (b) rGO(c) and (d)CBG-10 nanocomposite photocatalyst.

In the SEM morphological investigation, a reduced graphene oxide/biochar structure with a pleated laminar structure and a higher specific surface area could be seen (Fig. 3a). According to the results of the morphological analysis of the CBG-10 composite, the Co_3O_4 particles appear as equally sized, spherical

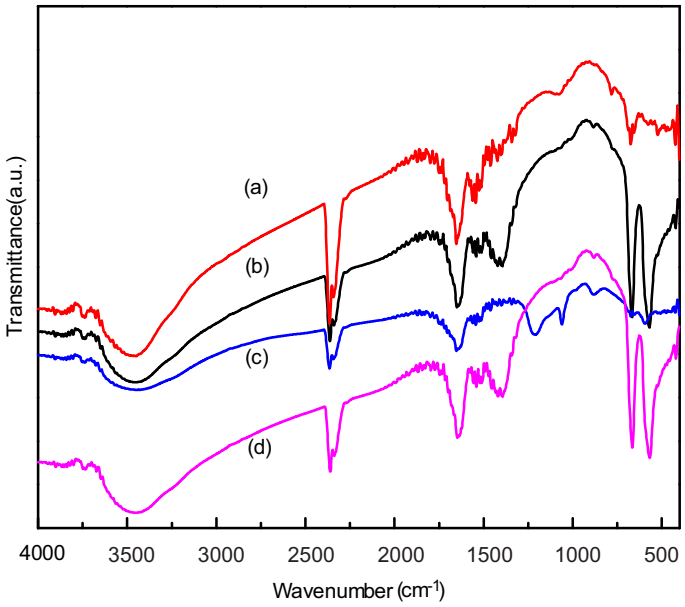

Fig. 2. FTIR analysis of (a) biochar(b)CBG-10(c)rGO and(d)Co_3O_4

dots that are evenly dispersed across the sheets of reduced graphene oxide and biochar. Therefore, the unique structure should have more surface active sites and a larger specific surface area. Co_3O_4 particles in the form of microspheres are seen to be exquisitely dispersed over graphene oxide and biochar. It describes how well they work together, showing that Co_3O_4 was successfully loaded onto graphene oxide / biochar. Numerous Co_3O_4 nanoparticles (shown as white dots in Figure 3(c) of CBG-10) are spread on the sheets of graphene oxide/biochar.

Test for photocatalytic activity: Fig. 4 depicts the photoactive degradation of MB/MG and the heavy metal Cr(VI) dye under visible light irradiation for 120 minutes while using the CBG-X catalyst. In a simple photoreactor, the photocatalyst (0.1 g) was suspended in 150 mL of a 20 mg/L dye aqueous solution to perform the photoreactions. Figure 5a shows that the percentage of degradation in the case of (rGO and biochar) was obtained at

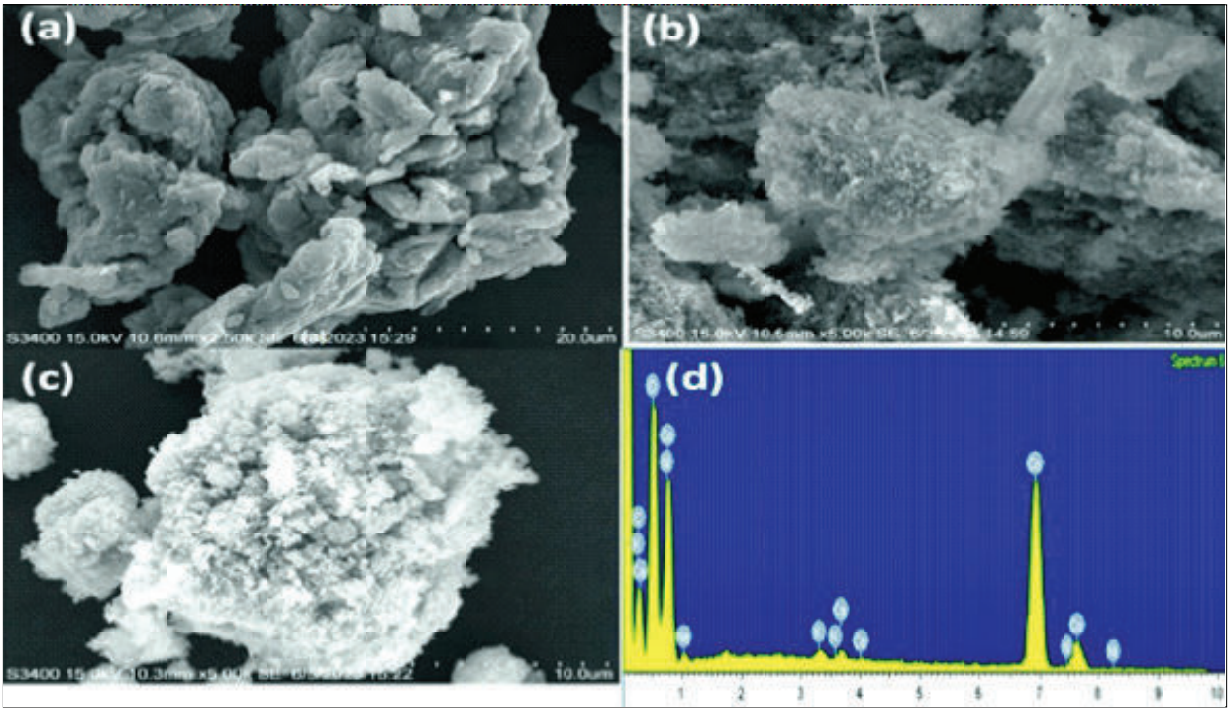

Fig. 3. SEM morphological study of the individual rGO/biochar (a), Co_3O_4(b) and synthesised CBG-10(c) (d)EDS of CBG-10

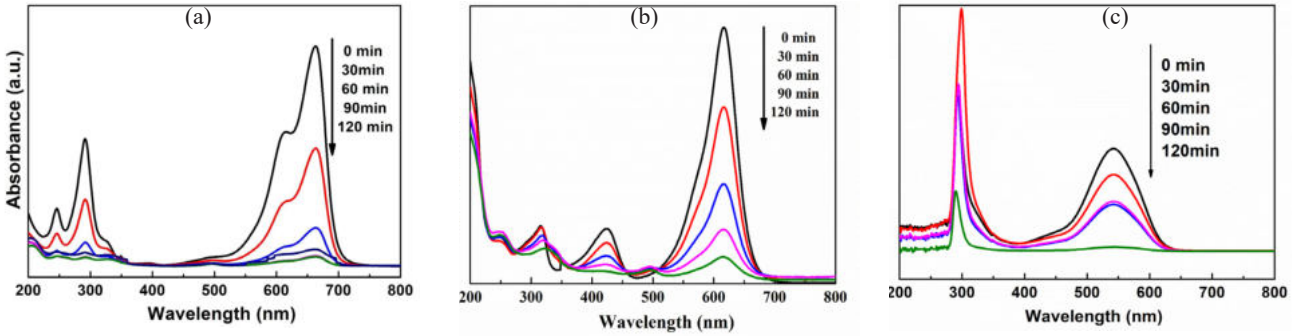

Fig. 4. UV-VIS spectrum analysis of MB(a), MG(b) and Cr(VI)(c)

10 weight percent, which is up to 100% with the illumination of light, and is better than the individual catalyst. Fig. 4(a-c) explains the degradation of the heavy metal Chromium (VI) and the MB/MG dye with time using CBG-10 from 0 to 120 minutes. On the contrary, Fig. 5(b) illustrates the progressive decline in absorbance intensity, indicating the complete degradation of the dye over an illumination period ranging from 0 to 120 minutes. This degradation process is likely attributed to the generation of

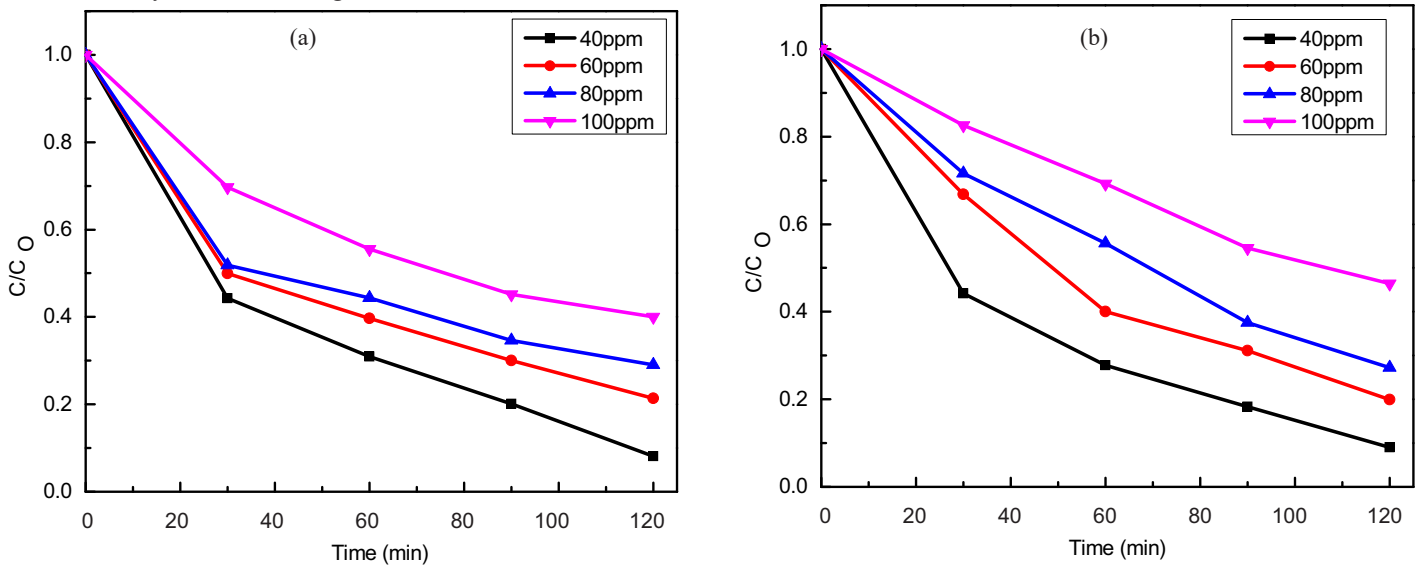

Fig. 5. Effect of illumination time of photodegradation of MG and MB at different initial concentrations by CBG-10.

active oxidants and reductants upon exposure to visible light, such as hydroxyl radicals, superoxide radicals, and holes (as shown in Fig. 5b). To elucidate the involvement of these reactive species in the photocatalytic degradation, experiments were conducted using different quenchers. The quenchers used in this reaction were 1 mm benzoquinone for trapping $^{o}O_2$ and 20 mL of isopropanol for trapping ^{o}OH and 1 mm of disodium EDTA for trapping h^+ (Jamil *et al.*, 2018). Because of this, photodegradation efficiency are reduced, which shows that superoxide radicals ($^{o}O_2$) and holes (h^+) are involved in the photodegradation of MG and MB.

In this experiment, we synthesised a CBG-10 composite using a quick, in-situ hydrothermal method. With exposure to visible light, this synthesised composite catalyst develops adequate catalytic action for the degradation of textile colours. In the presence of visible light, the CBG-10 catalyst totally up to 100% degraded the dye pollutant. Individual biochar/rGO and Co_3O_4 catalysts lack the chemical interaction that considerably boosts the stability and activity of the heterostructure. To explain it another way, the heterostructured Z-scheme photocatalysts driven by visible light are rather stable, which encourages higher reactivity, making them a capable substance for photocatalysis to offer relevant energy and environmental waste cleanup. The recyclability of CBG-10 was examined for successive four cycles, where it exhibits very minimal decrease in the percentage of dye degradation (< 5%) after four cycles indicating the stability as well as retaining the activity of the photocatalyst. In summary, an inexpensive hydrothermal reaction system was used to synthesise a CBG-10 composite. The phase and optical characteristics of the synthesised samples are confirmed using characterisation techniques. In contrast to their individual forms, the CBG-10 system exhibits considerable activity. In the presence of visible light exposure, the composite with a 10wt % biochar/rGO ratio displayed better photodegradation efficacy up to 100% for MB, MG dye, and heavy metal Cr(VI). This behaviour of the CBG-10 catalyst may be attributed to its excellent light absorption, Z-scheme band alignment, and effective e^-/h^+ migration, respectively. This study may lead to the creation of a novel CBG-10 photocatalyst for wastewater treatment and other environmental cleanup procedures.

Competing interests: The authors declare there are no competing interests

Acknowledgements

Amrita priyadarsini is very grateful to the ouat university for the support This work was supported by Department of Chemistry, Utkal University, Odisha.

Reference

Bankole, O.M., S.E. Olaseni, M.A. Adeyemo and A. S. Ogunlaja, 2020. Microwave-assisted synthesis of cobalt oxide/reduced graphene oxide (Co_3O_4–rGo) composite and its sulfite enhanced photocatalytic degradation of organic Dyes. *Zeitschrift für Physikalische Chemie*, 234(10): 1681-1708.

Bedia, J., V. Muelas Ramos, M. Peñas Garzón, A. Gómez Avilés, J. J. Rodríguez and C. Belver, 2019. A review on the synthesis and characterization of metal organic frameworks for photocatalytic water purification. *Catal.*, 9(1): 52.

Han, C., L. Ge, C. Chen, Y. Li, X. Xiao, Y. Zhang and L. Guo, 2014. Novel visible light induced Co_3O_4-g-C_3N_4 heterojunction photocatalysts for efficient degradation of methyl orange. *Appl. Catal. B: Environ.*, 147: 546-553.

Jamil, S., H. Ahmad, S.R. Khan and M.R.S.A Janjua, 2018. The first morphologically controlled synthesis of a nanocomposite of graphene oxide with cobalt tin oxide nanoparticles. *RSC Adv.*, 8(64): 36647-36661.

Koli, P. B., K.H. Kapadnis, U.G. Deshpande and M.R. Patil, 2018. Fabrication and characterization of pure and modified Co_3O_4 nanocatalyst and their application for photocatalytic degradation of eosine blue dye: a comparative study. *J. Nanostructure Chem.*, 8: 453-463.

Liao, L.B., Q. H. Zhang, Z.H. Su, Z.Z. Zhao, Y. N. Wang, Y. Li, X.X. Lu, D.G. Wei, G.Y. Feng, Q. K. Yu, X.J. Cai, J.M. Zhao, Z.F. Ren, H. Fang, F. Robles-Hernandez, S. Baldelli, J.M. Bao, 2014 Efficient solar water-splitting using a nanocrystalline CoO photocatalyst, *Nat. Nanotechnol*., 9: 69-73.

Laguna-Marco, M. A., D. Haskel, N. Souza-Neto, J. C. Lang, V. V. Krishnamurthy and M. van Veenendaal, 2010. Orbital magnetism and spin-orbit effects in the electronic structure of BaIrO 3. *PRL.*, 105(21): 216407.

Lester, E. D., G. Aksomaityte, J. Li, S. Gomez, J. Gonzalez-Gonzalez and M. Poliakoff, 2012. Controlled continuous hydrothermal synthesis of cobalt oxide (Co3O4) nanoparticles. *Prog. Cryst. Growth Charact. Mater.*, 58(1): 3-13.

Li, S., T. Zhu, L. Dong, and M. Dong, 2018. Boosted visible light photodegradation activity of boron doped rGO/gC 3 N 4 nanocomposites: The role of C–O–C bonds. *New J. Chem.*, 42(21): 17644-17651.

Li, X., R. Shen, S. Ma, X. Chen and J. Xie, 2018. Graphene-based heterojunction photocatalysts. *Appl. Surf. Sci.*, 430: 53-107.

Liu, X., G.Li, C. Chen, X. Zhang, K. Zhou and X. Long, 2022. Banana stem and leaf biochar as an effective adsorbent for cadmium and lead in aqueous solution. *Sci. Rep.*, 12(1): 1584.

Luo, Y., J. Luo, W. Zhou, X. Qi, H. Zhang, Y.W. Denis and T. Yu, 2013. Controlled synthesis of hierarchical graphene-wrapped TiO 2@ Co 3 O 4 coaxial nanobelt arrays for high-performance lithium storage. *J. Mater. Chem. A.*, 1(2): 273-281.

Peng, W., H. Li, Y. Liu and S. Song, 2017. A review on heavy metal ions adsorption from water by graphene oxide and its composites. *J. Mol. Liq.*, 230: 496-504.

Pouretedal, H.R. and M. Kiyani, 2014. Photodegradation of 2-nitrophenol catalyzed by CoO, CoS and CoO/CoS nanoparticles. *J. Iran. Chem. Soc.*, 11: 271-277.

Suresh, R., R. Udayabhaskar, C. Sandoval, E. Ramírez, R. V. Mangalaraja, H. D. Mansilla and J. Yáñez, 2018. Effect of reduced graphene oxide on the structural, optical, adsorption and photocatalytic properties of iron oxide nanoparticles. *New J Chem.*, 42(11): 8485-8493.

Xu, C., P.R. Anusuyadevi, C. Aymonier, R. Luque and S. Marre,2019. Nanostructured materials for photocatalysis. *Chem Soc Rev.*, 48(14): 3868-3902.

Ye, S., G. Zeng, H. Wu, J. Liang, C. Zhang and J. Yu, 2019. The effects of activated biochar addition on remediation efficiency of co-composting with contaminated wetland soil. *Resour Conserv Recycl* ., 140: 278-285.

Yuan, W., D. Xie, Z. Dong, Q. Su, J. Zhang, G. Du, and B. Xu, 2013. Preparation of porous Co_3O_4 polyhedral architectures and its application as anode material in lithium-ion battery. *Mater. Lett.*, 97: 129-132.

Received: January, 2024; Revised: February, 2024; Accepted: February, 2024